Inference for Quantile Measures of Kurtosis, Peakedness and Tail-weight

Robert G. Staudte
La Trobe University, Melbourne, Australia*
23 July, 2014

^{*}Emeritus Professor Robert G. Staudte, Department of Mathematics and Statistics, La Trobe University, Melbourne, Vic. 3086 Australia, r.staudte@latrobe.edu.au

Abstract

Many measures of peakedness, heavy-tailedness and kurtosis have been proposed in the literature, mainly because kurtosis, as originally defined, is a complex combination of the other two concepts. Insight into all three concepts can be gained by studying Ruppert's ratios of interquantile ranges. They are not only monotone in Horn's measure of peakedness when applied to the central portion of the population, but also monotone in the practical tail-index of Morgenthaler and Tukey, when applied to the tails. Distribution-free confidence intervals are found for Ruppert's ratios, and sample sizes required to obtain such intervals for a pre-specified relative width and level are provided. In addition, the empirical power of distribution-free tests for peakedness and bimodality are found for symmetric beta families and mixtures of t distributions. An R script that computes the confidence intervals is provided in online supplementary material.

Keywords: bimodality; distribution-free methods; skewed-t distributions; Tukey's sparsity index; variance stabilizing transformations

1 INTRODUCTION

1.1 Background and summary

The meaning of kurtosis has long puzzled statisticians, ever since the standardized fourth moment definition was introduced by Pearson (1905) to help describe departures from normality. A century elapsed before its asymptotic distribution was derived by Pewsey (2005), although its sister sample skewness result was obtained much earlier in Gupta (1967). In the meantime, numerous other measures of kurtosis have been proposed and dissected, but again with almost no accompanying inferential methods.

There are three themes pervading research into kurtosis measures. Firstly, kurtosis as originally conceived is a location, scale and signinvariant measure of shape that somehow measures both peakedness and tail-weight. Contributions by many authors to this theme are thoroughly described by Balanda & Macgillivray (1988). Secondly, an increase in a kurtosis measure should quantify movement of mass from the tails to the center of the distribution, with substantive contributions from van Zwet (1964), Oja (1981) and Balanda & Macgillivray (1988, 1990). The third theme is that quantile-based measures are preferable to moment-based measures: they are always defined and are robust in that they have bounded influence functions and positive breakdown points. Contributions of this type include Groeneveld & Meeden (1984), Ruppert (1987), Moors (1988), Groeneveld (1998) and Kotz & Seier (2009). Also of interest are the maximum-bias curves for interguantile ranges studied by Croux & Haesbroeck (2001), the robust kurtosis measures of Seier & Bonett (2003), and the L-moment kurtosis measures of Withers & Nadarajah (2011).

Recently Jones et al. (2011) studied ratios of linear combinations of interquantile ranges, and showed that they possessed the surprising property of invariance to skewness-inducing transformations. The simplest measures of this type, ratios of two interquantile ranges, were introduced by Ruppert (1987), who compared their influence functions and order-preserving properties with other measures of kurtosis. Despite their simplicity, they provide a basis for studying the peakedness and tail-weight properties of distributions, separately or jointly.

As explained further in Section 2, these simple ratios measure peakedness when applied to the center of a distribution, and they measure tail-weight when applied to the remaining (tails) portion. This idea is already exploited by Schmid & Trede (2003), who found tests for normality based on these ratios of ranges. In Section 2.1 we extend the peakedness measure of Horn (1983) so that it can detect bimodality, and show that the Ruppert (1987) kurtosis, when applied to the central portion of the distribution, continues to be approximately monotone in it. We further show in Section 2.2 that, when applied to the tails portion, the Ruppert kurtosis is monotone in the index of tail-weight of Morgenthaler & Tukey (2000).

In Section 3 we briefly describe inference for the ratio of interquantile ranges when the underlying location-family is known; it is based on a variance stabilizing transformation (VST) which requires three constants, each depending on the family through the sparsity index of Tukey (1965). By estimating these constants (nuisance parameters), which requires density estimates at four quantiles, one obtains distribution-free confidence intervals for the ratio of interquantile

ranges. These intervals are evaluated by simulation studies for coverage and widths in Section 4. The coverage for 90% or 95% confidence intervals is accurate provided that the sample size is at least 400. The empirical power of the Ruppert measures for detecting peakedness and/or bimodality is also found for the symmetric Beta models and mixtures of t distributions. A summary and further research problems are outlined in Section 5.

1.2 Preliminary definitions and concepts

For any strictly increasing distribution function F and 0 < t < 1 let $x_t = G(t) \equiv F^{-1}(t)$ denote the tth quantile. For 0 < t < 0.5 denote the tth interquantile range of F by $R_t = R_t(F) = x_{1-t} - x_t$. Then for $0 Ruppert (1987) defined a measure of kurtosis by <math>\kappa_{p,r} = R_p/R_r$. (Our notation differs from his: our $\kappa_{p,r}$ is his $R_{r,p}$.) These measures are clearly sign, location and scale invariant. Our choice of (p,r) is guided by a desire to have a quantile measure which agrees at the normal model with the classical moment-based definition of kurtosis $\alpha_4(F) = \mu_4/\mu_2^2$, where $\mu_k = \mathrm{E}_F[(X - \mathrm{E}[X])^k]$, is the kth moment about the mean $\mathrm{E}_F[X]$, $k = 2, 3, \ldots$. The normal model $F = \Phi$ has $\alpha_4(\Phi) = 3$. In the case of symmetric F, $\kappa_{p,r} = x_p/x_r$, so to have $\kappa_{p,r} = 3$ for the normal distribution, we need to have $p = p(r) = \Phi(3\Phi^{-1}(r))$. Some examples are given in Table 1. Further, we want to be able to carry out tests and find confidence intervals for $\kappa_{p,r}$, and to provide some protection against outliers by choice of (p,r).

The models in Table 1 are labeled with standard notation in Johnson et al.

Table 1: Examples of the kurtosis coefficient $\kappa_{p,r} = R_p/R_r$, for various models and four choices of (p(r), r), with r = 0.3, 0.333, 0.35, 0.4 and $p(r) = \Phi(3\Phi^{-1}(r))$. Also shown is the classical kurtosis $\alpha_4(F)$.

\overline{F}	$\alpha_4(F)$	r = 0.3	r = 1/3	r = 0.35	r = 0.4
1. $Beta(1/2, 1/2)$	1.50	1.673	1.906	2.038	2.470
2. Uniform	1.80	2.211	2.411	2.508	2.764
3. $Beta(2,2)$	2.14	2.588	2.709	2.762	2.892
4. Normal	3.00	3.000	3.000	3.000	3.000
5. Logistic	4.20	3.294	3.200	3.160	3.070
6. Student- t_5	9.00	3.399	3.260	3.205	3.086
7. Student- t_4	_	3.523	3.337	3.265	3.110
8. Student- t_2	_	4.340	3.820	3.631	3.250
9. Laplace	6.00	4.223	4.016	3.913	3.606
10. Cauchy	_	7.492	5.438	4.787	3.635
11. $Beta(2,1)$	2.40	2.527	2.661	2.722	2.872
12. χ_5^2	5.40	3.088	3.060	3.048	3.021
13. χ_3^2	7.00	3.167	3.113	3.091	3.039
14. χ_2^2	9.00	3.293	3.200	3.161	3.070
15. χ_1^2	15.00	3.881	3.625	3.511	3.232
16. Log-normal	113.94	4.205	3.789	3.624	3.262
17. Skew- $t_{2,2}$	_	4.340	3.820	3.631	3.250
18. Pareto(2)	_	4.961	4.216	3.941	3.377
19. Skew- $t_{2,1}$	_	7.492	5.438	4.787	3.635
20. Skew- $t_{2,1/2}$	_	30.452	14.033	10.189	4.984

(1994, 1995), but two cases require clarification: the Pareto distribution with shape parameter a=2 has distribution function given by $F(x)=1-1/x^2$ for $x\geq 1$. The class of 'skewed-t' distributions introduced by Rosco et al. (2011) are denoted $t_{\epsilon,\nu}$ where ϵ is a real skewness parameter and $\nu>0$ is the degrees of freedom. If $X\sim t_{\nu}$, then $Y=\sinh(\sinh^{-1}(X)+\epsilon)\sim t_{\epsilon,\nu}$. Clearly $t_{0,\nu}=t_{\nu}$ and $t_{\epsilon,+\infty}$ is the skewed normal model, while $t_{\epsilon,1}$ is the skewed Cauchy model. A nice property of these distributions is that ratios of linear combinations of interquantile ranges are not dependent on the skewness parameter ϵ , see Jones et al. (2011). However, as shown in Section 4, $\kappa_{p,r}(t_{\epsilon,1})$ is much more difficult to estimate for $\epsilon=2$ than $\epsilon=0$.

The second column of Table 1 gives values of the classical moment kurtosis for the Models in Column 1. The remaining columns give values of $\kappa_{p(r),r}$ for r=0.3,1/3,0.35,0.4. Note that the kurtosis $\kappa_{p(r),r}$ becomes more discriminating as r gets smaller; however even for r=0.25, the value of p(r) is 0.0215, so r<0.3 is excluded to guarantee resistance to 5% of outliers. As $r\to0.5$, $\kappa_{p(r),r}\to3$, by L'Hospital's rule. Therefore larger values of $r\geq0.4$ are less informative. Within the range $0.3\leq r\leq0.4$ we decided to focus on r=1/3 because then the ordering of $\kappa_{1/3}=\kappa_{p(1/3),1/3}(F)$ for the various models F in Table 1 is roughly consistent with that of $\alpha_4(F)$, as well as agreeing exactly at $F=\Phi$. Further, it is easy to remember that because $p(1/3)\approx0.1$, one is comparing the range of the middle 4/5 of the population with the range of the middle 1/3.

2 PEAKEDNESS AND TAILWEIGHT

Throughout this section fix 0 . The 'central' portion of the distribution of <math>F is that lying between x_q and x_{1-q} while the 'tail' portion is that lying outside these quantiles. We will show that applying the kurtosis measure of Ruppert (1987) to the center of the distribution leads to a peakedness measure, while applying it to the tails portion leads to a tail-weight measure. To this end, define the (central) quantile peakedness by $\pi_{q,r} = R_q/R_r$, for q < r < 0.5. Define the quantile tail-weight by $\tau_{p,q} = R_p/R_q$, for $0 . Trivially, the product is the 'kurtosis' measure <math>\kappa_{p,r} = \tau_{p,q} \pi_{q,r} = R_p/R_r$ for the distribution F. All three measures satisfy the kurtosis convexity criterion of van Zwet (1964) and that of Lawrence (1975), see (Ruppert, 1987, Theorem 2). And each has the simplest form of a skewness invariant kurtosis measures (Jones et al., 2011, Sec. 2.1).

Schmid & Trede (2003) carried out tests for peakedness, tail-weight and leptokurtosis based on sample versions of $\pi_{q,r}$, $\tau_{p,q}$ and $\kappa_{p,r}$, respectively, for the case of p=1/40, q=1/8 and r=1/4 (our notation). We prefer larger values because their choice of r=1/4 means that the central half of the data are ignored in assessing peakedness. Further, their choice of p=1/40 means that the breakdown point of the procedure is only 1/40. In any case, their emphasis is on testing while ours is on confidence intervals so the results to follow can be seen as complementary to theirs.

2.1 Peakedness Measures

A justification for calling $\pi_{q,r} = R_q/R_r$ quantile peakedness for symmetric unimodal distributions is already given by Ruppert (1987). He showed that for r less than, but near 0.5, $\pi_{q,r}$ is approximately monotone increasing in the peakedness measure of Horn (1983). However, Horn only considered symmetric densities f that were unimodal. Next we extend his measure of central peakedness to one that distinguishes bimodality and show that $\pi_{q,r}$ is still approximately monotone increasing in this extended version.

A simple extension of Horn's measure of peakedness

Horn (1983) considered densities such as that depicted in the upper left plot of Figure 1. Consider the rectangle with base $[x_q, x_{1-q}]$ and height $f(x_{0.5})$ which has area $A_q = f(x_{0.5})R_q$; then Horn's measure (our notation) is based on the ratio $(1-2q)/A_q$, which for symmetric unimodal f is the proportion of the area of the rectangle which lies under the density. Clearly this ratio, which lies between 0 and 1, will be *smaller* with more peakedness. To make it increasing in peakedness, Horn (1983) defined $\eta_q = 1 - (1-2q)/A_q$, which still varies from 0 to 1, but now with *larger* values indicating more peakedness.

At the other extreme, the bottom left plot in Figure 1 indicates that symmetric U-shaped distributions with minimum at the median will have the ratio $(1-2q)/A_q > 1$. These observations motivate a measure of (central) peakedness defined by

$$\eta_q = \begin{cases} -1 + A_q/(1 - 2q) & \text{for } A_q \le (1 - 2q) ; \\ +1 - (1 - 2q)/A_q, & \text{for } (1 - 2q) \le A_q . \end{cases}$$
 (1)

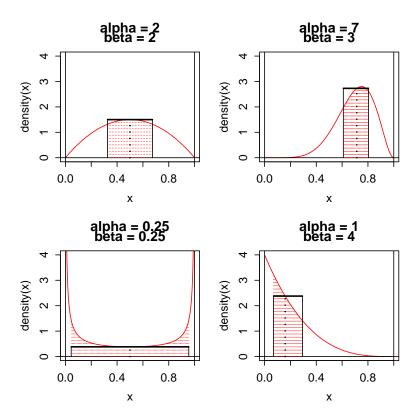


Figure 1: In these plots q=1/4. Four Beta (α,β) densities are shown, with parameters listed above each plot. The areas lying under the densities and over the interval $[x_q,x_{1-q}]$ are shaded and have areas equal to 1-2q=1/2. These are to be compared to the areas of the rectangles $A_q=f(x_{0.5};\alpha,\beta)$ $R_{1/4}(\alpha,\beta)$. The respective medians are marked by the vertical dotted lines. See text for more details.

This η_q agrees with Horn's definition for symmetric unimodal f, but can be applied to arbitrary f, even if $f(x_{0.5}) = 0$ or $+\infty$. It lies in [-1,1], takes on negative values for symmetric U-shaped models, and equals 0 for the uniform distribution.

Some examples of η_q for q=1/4 are shown in Figure 2, where its graph is plotted as a solid line for the Beta (β,β) , $\beta>0$ family; a

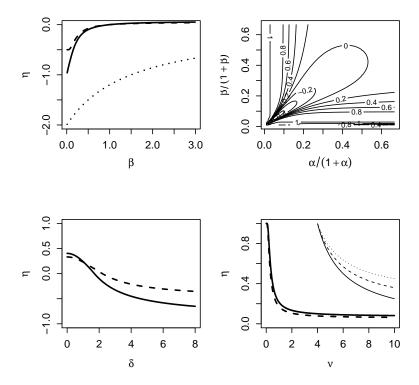


Figure 2: In these plots q=1/4 and r=3/8. In the top left plot is shown the graph of η_q defined in (1) as a function of β for the Beta(β , β) model as a thick solid line. Its approximation $\hat{\eta}_{q,r}$ is plotted as a thick dashed line. The dotted line shows the graph of α_4-3 . In the upper right plot are shown contours of η_q for the Beta(α , β) model. Note that it takes on negative values within the contour marked 0. The bottom left plot again shows η_q and its approximation $\hat{\eta}_{q,r}$ for a 50:50 mixture of two $t_{1/2}$ distributions that are distance δ apart. The bimodality is detected in that $\eta_q < 0$ for $\delta > 1.5$. The approximation of η_q by $\hat{\eta}_{q,r}$ improves as r moves closer to 0.5. The bottom right plot shows η_q and its approximation as functions of ν for the skew- $t_{\epsilon,\nu}$ distributions; it does not depend on ϵ . Also shown are values of $(\alpha_4 - 3)/\alpha_4$ for $\epsilon = 0$, 0.25, and 1, respectively in thin solid, dashed and dotted lines.

50:50 mixture of two Student- $t_{1/2}$ models, one of which is shifted by $\delta > 0$, and the skew- $t_{\epsilon,\nu}$ families for $0 < \nu < 10$ and selected values of ϵ . Also shown is a contour plot of η_q for the Beta (α, β) family, $\alpha > 0, \beta > 0$. These plots confirm that η_q can detect bimodality as well as peakedness.

The measure $\pi_{q,r}$ is monotone increasing in η_q .

An approximation to η_q can be obtained as in Ruppert (1987): for small $\epsilon > 0$ one has the finite difference approximation $f(x_{0.5}) \approx 2\epsilon/\{x_{0.5+\epsilon} - x_{0.5-\epsilon}\}$. Thus for 0 < q < r < 0.5 and r near 0.5, say $\epsilon = 0.5 - r$,

$$\frac{A_q}{(1-2q)} \approx \frac{(1-2r)R_q}{(1-2q)R_r} = c_{q,r}\pi_{q,r} , \qquad (2)$$

where $c_{q,r} = (1-2r)/(1-2q) < 1$. Hence $\pi_{q,r} \approx \hat{\pi}_{q,r} \equiv A_q/(1-2r)$ is approximately monotone increasing in the peakedness measure η_q , justifying the name 'measure of peakedness'. Substitution of $c_{q,r}\hat{\pi}_{q,r}$ for $A_q/(1-2q)$ in (1) yields an approximation for $\eta_{q,r}$ that is hereafter denoted $\hat{\eta}_{q,r}$. Examples are shown as thick dashed lines in Figure 2.

2.2 Tail-weight Measures

To justify calling $\tau_{p,q}$ a tail-weight measure, recall that F has a right tail with (asymptotic) index $\alpha_R > 0$ if $1-F(x) \sim u(x)x^{-\alpha_R}$ as $x \to \infty$, where u(x) is a slowly varying function. Noting that density estimation for wide-tailed distributions is difficult, Morgenthaler & Tukey (2000) introduce what they call a 'practical tail index', which, in our notation, for $0 is the ratio <math>\alpha_R(p,q) = \ln(q/p)/\ln(x_{1-p}/x_{1-q})$. They explain why this gives a good indication of the size of α_R , espe-

cially when computed for a range of pairs (p,q). Similarly, if the left tail index is denoted α_L , one can derive $\alpha_L(p,q) = \ln(q/p)/\ln(x_p/x_q)$. It follows that $x_p = x_q (q/p)^{1/\alpha_L(p,q)}$ and $x_{1-p} = x_{1-q} (q/p)^{1/\alpha_R(p,q)}$, so that

$$\tau_{p,q} = \frac{R_p}{R_q} = \frac{x_{1-q} \left(\frac{q}{p}\right)^{1/\alpha_R(p,q)} - x_q \left(\frac{q}{p}\right)^{1/\alpha_L(p,q)}}{x_{1-q} - x_q} \ . \tag{3}$$

This expression shows how the left and right hand practical tail indices affect $\tau_{p,q}$. For example as $\alpha_R(p,q)$ grows large, indicating a short right tail, the first term in the numerator of (3) approaches x_{1-q} , the first term in the denominator. But if $\alpha_R(p,q)$ decreases, the same first term of the numerator becomes larger than the first term below it. Similar remarks can be made for the left tail, but the main point is the $\tau_{p,q}$ increases as either of the practical tail indices decrease, as one would expect of a measure of tail-weight.

For symmetric distributions, $\alpha_L(p,q) = \alpha_R(p,q) \equiv \alpha(p,q)$, so $\tau_{p,q} = (q/p)^{1/\alpha(p,q)}$. Morgenthaler & Tukey (2000) give examples, including the Student- t_{ν} distribution which has tail index $\alpha = \nu$, and their H_h distributions for which $\alpha = 1/h$. For such distributions moments of larger order than α do not exist.

2.3 Examples of Peakedness and Tail-weight

A distribution-free choice for partitioning the distribution is $x_{0.125}$, $x_{0.25}$ and $x_{0.375}$, so that comparisons are made between the ranges of the central quarter, half and three-quarters of the population. Table 2 tabulates values of $\pi_{q,r}$, $\tau_{p,q}$ and $\kappa_{p,r}$ for this partition; that is, for p = 1/8, q = 1/4 and r = 3/8. The symmetric models are listed in terms

of increasing values of $\kappa_{p,r}$ and similarly for the asymmetric models. Note that peakedness $\pi_{q,r}$ contributes more than tail-weight $\tau_{p,q}$ for all models except Models 10, 20 and 21. Models 10, the Cauchy, and the skewed Cauchy $t_{2,1}$ have identical values and peakedness and tail-weight contribute equally to kurtosis for each of them, as guaranteed by the results in Jones $et\ al.\ (2011)$. Only Model 21, the very skewed $t_{2,1/2}$ family, has a larger tail-weight than peakedness.

Perhaps it is worth noting that the peakedness of t_{ν} and χ^{2}_{ν} models increases with decreasing ν , as one would expect from comparison of graphs of their densities. The only drawback of these definitions in terms of the ranges of the middle quarter, half and three-quarters of the population is that the kurtosis for the normal model does not agree with the classical measure; here the uniform model has kurtosis equal to 3. Also, for the normal model there is not much difference between the peakedness and tail-weight, and traditionalists might expect that tail-weight should contribute much less than peakedness, because the normal model has relatively short tails.

A Gaussian-centric choice could define the central portion of the distribution as that lying within one standard deviation of the mean; that is, $q = \Phi^{-1}(-1) = 0.1586553$. Then, taking r = 1/3 and $p = \Phi(3\Phi^{-1}(r)) = 0.098 \approx 0.1$ for reasons given in Section 1 gives somewhat different results, also listed in Table 2. Now the kurtosis for the normal is 3 by definition, and the contribution of its peakedness factor is almost twice that of tail-weight. In fact the contribution of peakedness to tail-weight has increased for all distributions. Nevertheless, the orderings of kurtosis within symmetric and asymmetric groups remains unchanged from the 'model-free' choice of p, q and r.

Table 2: Columns 2-4 give the quantile peakedness $\pi_{q,r}$, the quantile tail-weight $\tau_{p,q}$ and their product, the kurtosis $\kappa_{p,r}$, for various models F when p=1/8, q=1/4 and r=3/8. Columns 5-7 contain the corresponding values when r=1/3, $p=\Phi(3\Phi^{-1}(r))\approx 0.1$, $q=\Phi^{-1}(-1)\approx 0.158$.

F	$\pi_{q,r}$	$ au_{p,q}$	$\kappa_{p,r}$	$\pi_{q,r}$	$ au_{p,q}$	$\kappa_{p,r}$
1. $Beta(1/2, 1/2)$	1.848	1.307	2.414	1.757	1.085	1.906
2. Uniform	2.000	1.500	3.000	2.048	1.177	2.411
3. $Beta(2,2)$	2.064	1.606	3.316	2.193	1.235	2.709
4. Normal	2.117	1.706	3.610	2.322	1.292	3.000
5. Logistic	2.151	1.771	3.809	2.407	1.330	3.200
6. Student- t_5	2.158	1.790	3.864	2.429	1.342	3.260
7. Student- t_4	2.170	1.815	3.938	2.460	1.357	3.337
8. Student- t_2	2.236	1.964	4.392	2.643	1.446	3.820
9. Laplace	2.409	2.000	4.819	2.831	1.418	4.015
10. Cauchy	2.414	2.414	5.828	3.182	1.709	5.438
11. $Beta(2,1)$	2.054	1.590	3.265	2.170	1.226	2.661
12. χ_5^2	2.127	1.725	3.669	2.347	1.304	3.060
13. χ_3^2	2.136	1.743	3.722	2.370	1.314	3.113
14. χ_2^2	2.151	1.771	3.809	2.407	1.330	3.200
15. χ_1^2	2.229	1.906	4.249	2.595	1.397	3.625
16. Log-normal	2.243	1.956	4.386	2.646	1.432	3.789
17. Skew- $t_{2,2}$	2.236	1.964	4.392	2.643	1.446	3.820
18. $Pareto(2)$	2.296	2.081	4.780	2.800	1.506	4.216
19. Skew- $t_{2,1}$	2.414	2.414	5.828	3.182	1.709	5.438
20. Skew- $t_{2,1/2}$	2.996	4.222	12.649	5.329	2.633	14.033

3 DISTRIBUTION-FREE INFERENCE

The material in this section focusses on the kurtosis coefficient $\kappa_{p,r}$, but equally applies to peakedness $\pi_{q,r}$ or tail-weight $\tau_{p,q}$. Let $X_{([nr])}$ denote the [nr]th order statistic of a sample of size n from F, and define the sample version of R_r by $\hat{R}_r = R_r(F_n) = X_{(n-[nr]+1)} - X_{([nr])}$. We estimate $\kappa_{p,r} = R_p/R_r$ by $\hat{\kappa}_{p,r} = \hat{R}_p/\hat{R}_r$.

3.1 Variance Stabilization of $\hat{\kappa}_{p,r}$

The methodology for finding a variance stabilizing transformation (VST) of a ratio of statistics, each of which is a finite linear combination of order statistics, has already been established for other ratios of linear combinations of quantiles in Staudte (2013a,b, 2014), so here we only restate the required results. One first shows that $\operatorname{Var}[\hat{\kappa}_{p,r}] = \operatorname{Var}[\hat{R}_p/\hat{R}_r]$ satisfies $\operatorname{Var}[\hat{\kappa}_{p,r}] \doteq \operatorname{Var}[\hat{R}_p - \operatorname{E}[\hat{\kappa}_{p,r}]\hat{R}_r]/R_r^2$. Therefore $n\operatorname{Var}[\hat{\kappa}_{p,r}] = q(\operatorname{E}[\hat{\kappa}_{p,r}])$ where $q(t) = a_0 + a_1t + a_2t^2$ is a quadratic with constants:

$$a_0 = a_0(p,r) = n \text{Var}_F[\hat{R}_p]/R_r^2$$

 $a_1 = a_1(p,r) = -2n \text{Cov}_F[\hat{R}_p, \hat{R}_r]/R_r^2$ (4)
 $a_2 = a_2(r) = n \text{Var}_F[\hat{R}_r]/R_r^2$.

Note that a_0 , a_1 and a_2 are free of location, scale and sample size. The quadratic q(t) > 0 for all t because $a_0 > 0$ and its discriminant $a_1^2 - 4a_0a_2 < 0$; the latter inequality follows from $|a_1/\{2\sqrt{a_0a_2}\}| = |\operatorname{Corr}[\hat{R}_p, \hat{R}_r]| < 1$. Hereafter let $D^2 = 4a_0a_2 - a_1^2$. In the remainder of this subsection, drop the subscripts p, r on $\kappa_{p,r}$. A variance stabilizing

transformation (VST) of $\hat{\kappa}$ is

$$h_n(x) = \sqrt{\frac{n}{a_2}} \sinh^{-1} \left\{ \frac{q'(x)}{D} \right\} + c ,$$
 (5)

where c is an arbitrary real number. In carrying out inference for κ , it is useful to center $h_n(\hat{\kappa})$ at an arbitrary null hypothesis value $\kappa_0 \geq 1$ by introducing $T_{n,\kappa_0}(\hat{\kappa}) = h_n(\hat{\kappa}) - h_n(\kappa_0)$, so $\mathbf{E}_{\kappa_0}[T_{n,\kappa_0}]$ is approximately 0 under the null. By the Delta Theorem (DasGupta, 2006, p.40), as n grows without bound, $T_{n,\kappa_0}(\hat{\kappa}) \sim N(\sqrt{n} K_{\kappa_0}(\kappa), 1)$, where

$$K_{\kappa_0}(\kappa) = \frac{1}{\sqrt{a_2}} \left[\sinh^{-1} \left\{ \frac{q'(\kappa)}{D} \right\} - \sinh^{-1} \left\{ \frac{q'(\kappa_0)}{D} \right\} \right] . \tag{6}$$

We can write $T_{n,\kappa_0}(\hat{\kappa}) = \sqrt{n} K_{\kappa_0}(\hat{\kappa})$. A level- α test rejects the null $\kappa = \kappa_0$ in favor of $\kappa > \kappa_0$ for $T_{n,\kappa_0}(\hat{\kappa}) \ge z_{1-\alpha} = \Phi^{-1}(1-\alpha)$.

To make this statistic distribution-free, the nuisance parameters a_0 , a_1 and a_2 must be estimated. They depend on the unknown F through the sparsity index $g_p = g(p) = 1/f(x_p)$ of Tukey (1965), at each of the quantiles $x_p < x_r < x_{1-r} < x_{1-p}$. This requires density estimates at the selected quantiles, and the resulting constants are denoted \hat{a}_0 , \hat{a}_1 and \hat{a}_2 . When these estimated constants are substituted into q, D, and $T_{n,\kappa_0}(\hat{\kappa}) = \sqrt{n} K_{\kappa_0}(\hat{\kappa})$, the results are denoted \hat{q} , \hat{D} and $T_{\mathrm{DF},n,\kappa_0}(\hat{\kappa})$. The method of sparsity density estimation described in (Staudte, 2014, Sec. 4.1) is also utilized here; but the constants (7) are different in this kurtosis setting.

3.2 Constants required by the VST

For fixed $0 < r \le s < 1$ and sample size n increasing without bound, $\mathrm{E}[X_{([nr]]}] \doteq x_r$ and $n\mathrm{Cov}[X_{([nr]}, X_{([ns]]}] \doteq r(1-s)g_rg_s$, where ' \doteq '

means that lower order terms are ignored; see, eg. (David, 1981, p.80) or (DasGupta, 2006, p.93).

It follows that for 0 the constants (4) required by the VST are:

$$R_r^2 a_0(p,r) = p(g_p^2 + g_{1-p}^2) - p^2(g_p + g_{1-p})^2$$

$$R_r^2 a_1(p,r) = 2\{pr(g_r g_{1-p} + g_p g_{1-r}) - p(1-r)(g_p g_r + g_{1-p} g_{1-r})\}$$

$$R_r^2 a_2(r) = r(g_r^2 + g_{1-r}^2) - r^2(g_r + g_{1-r})^2.$$
(7)

When F is symmetric, $R_r = 2x_{1-r}$ and $g_r = g_{1-r}$, so these formulae reduce to $a_0(p,r) = 2p g_p^2/R_r^2$, $a_1(p,r) = 4p g_p g_r (2r-1)/R_r^2$ and $a_2(r) = 2r g_r^2/R_r^2$. Table 3 lists values of $\kappa_{1/3} = \kappa_{p(1/3),1/3}$, where $p(r) = \Phi(3\Phi^{-1}(r))$, and the VST constants a_0 , a_1 and a_2 .

3.3 Two-sided Confidence Intervals for κ

A nominal $100(1 - \alpha)\%$ distribution-free confidence interval for κ is derived exactly as for the skewness coefficient in (Staudte, 2014, Sec. 3.3) and displayed in Equation 9 of that paper; its analogue here is, for $c_{\alpha} = z_{1-\alpha/2}$:

$$[L, U]_{DF} = \frac{1}{\hat{a}_2} \left[\hat{D} \sinh \left\{ \sinh^{-1} \left(\frac{\hat{q}'(\hat{\kappa})}{\hat{D}} \right) \pm c_\alpha \sqrt{\frac{\hat{a}_2}{n}} \right\} - \hat{a}_1 \right] . \quad (8)$$

In this expression \hat{a}_0 , \hat{a}_1 and \hat{a}_2 as well as \hat{q}' and \hat{D} are all estimated using distribution-free methods. The empirical coverage of nominal 90% and 95% distribution-free confidence intervals for κ based on (8) are found for various n in Section 4. Also of interest are the widths of these intervals, defined by $W = U_{DF} - L_{DF}$.

Table 3: For r=1/3 and $p=\Phi(3\Phi^{-1}(r))=0.1$ are listed the kurtosis coefficient $\kappa_{1/3}=R_p/R_r$, the VST constants (4), the asymptotic width $w_{asym}=2\sqrt{q(\kappa_{1/3})}$ appearing in (9) and the asymptotic relative widths $rw_{asym}=w_{asym}/\kappa_{1/3}$.

F	$\kappa_{1/3}$	a_0	a_1	a_2	w_{asym}	rw_{asym}
1. $Beta(1/2, 1/2)$	1.906	0.143	-0.339	1.645	4.678	2.455
2. Uniform	2.411	1.420	-1.178	2.000	6.390	2.650
3. $Beta(2,2)$	2.709	3.512	-1.919	2.146	7.499	2.770
4. Normal	3.000	7.094	-2.802	2.265	8.735	2.912
5. Logistic	3.200	10.478	-3.462	2.342	9.670	3.022
6. Student- t_5	3.260	11.882	-3.699	2.358	9.975	3.060
7. Student- t_4	3.337	13.646	-3.986	2.384	10.371	3.108
8. Student- t_2	3.820	28.436	-5.930	2.531	13.073	3.422
9. Laplace	3.200	20.049	-5.772	3.752	12.648	3.953
10. Cauchy	5.438	137.680	-14.024	2.924	24.323	4.473
11. $Beta(2,1)$	2.661	4.088	-2.261	2.311	7.599	2.856
12. χ_5^2	3.060	10.939	-3.931	2.543	9.532	3.115
13. χ_3^2	3.113	14.104	-4.857	2.773	10.171	3.267
14. χ_2^2	3.200	18.899	-6.244	3.122	11.115	3.474
15. χ_1^2	3.625	41.492	-12.353	4.660	15.226	4.200
16. Log-normal	3.789	49.077	-11.552	3.811	15.495	4.089
17. Skew- $t_{2,2}$	3.820	54.245	-12.480	3.943	16.014	4.192
18. Pareto(2)	4.216	90.352	-17.572	4.496	19.616	4.652
19. Skew- $t_{2,1}$	5.438	282.221	-32.651	4.963	31.712	5.831
20. Skew- $t_{2,1/2}$	14.033	6958.645	-218.133	8.456	149.167	10.630

They can be expressed, see (Staudte, 2014, App.2),

$$W = \frac{w_{asym}(\hat{\kappa}) z_{1-\alpha/2}}{\sqrt{n}} + o_p(n^{-1/2}) , \qquad (9)$$

where $w_{asym}(\kappa) = 2\sqrt{q(\kappa)}$ and $q(t) = a_0 + a_1 t + a_2 t^2$. Thus for large n the half-width of the confidence intervals (8) is approximately $z_{1-\alpha/2}$ times the standard error of $\hat{\kappa}$, which is $\sqrt{\operatorname{Var}[\hat{\kappa}]} \approx \sqrt{q(\kappa)/n}$.

Since $\hat{\kappa}$ is consistent for κ it is of interest to evaluate $2\sqrt{q(\kappa)}$ for various F. It turns out that the interval widths are almost linearly increasing with κ , so we also introduce the relative width $rW = W/\kappa$. It follows from (9) that to obtain a large sample $100(1-\alpha)\%$ confidence interval for κ of desired relative width $rW_0 = W_0/\kappa$ one requires

$$n \ge n_0 = n_0(\alpha, rW_0) = \left\{ \frac{\max_F \{ rw_{asym}(F) \} \ z_{1-\alpha/2}}{rW_0} \right\}^2 . \tag{10}$$

where $rw_{asym}(F) = 2\sqrt{q(\kappa(F))}/\kappa(F)$. By referring to Table 3, one sees that for the choices r = 1/3, q = 1/10, excluding the skew-t distributions, $rw_{asym}(F) \leq 4.652$. To ensure $rW_0 = 0.2$ with 95% confidence, one requires $n \geq n_0 = (4.652 \times 1.96 \times 5)^2 = 2079$.

4 SIMULATION RESULTS

4.1 Empirical Coverage and Widths

We find distribution-free confidence intervals for $\kappa = \kappa_{p(r),r}$, where r = 1/3 and $p(r) = \Phi(3\Phi^{-1}(r)) \approx 0.1$, for reasons given in Section 1. In our simulation studies we used the software package R Team (2008), and estimated the sparsity index using the method described in (Staudte, 2014, Sec.4).

Table 4: Estimates of coverage probabilities and widths of nominal 90% and 95% confidence intervals for $\kappa_r = \kappa_{p(r),r}$ when r = 1/3 and $p(r) = \Phi(3\Phi^{-1}(r)) = 0.09815$, all based on 40,000 replications of samples from selected symmetric models. The average interval relative widths are not shown but can be recovered from $\overline{rW} = \widehat{rw} \ z_{1-\alpha/2}/\sqrt{n}$, see (9).

	90%				95%			
F	n	$\hat{\kappa}_{1/3}$	cp	\widehat{rw}	n	$\hat{\kappa}_{1/3}$	cp	\widehat{rw}
	100	2.454	0.918	2.874	100	2.454	0.961	2.887
2. Uniform	400	2.421	0.906	2.715	400	2.421	0.954	2.719
	1000	2.415	0.904	2.679	1000	2.415	0.953	2.680
	4000	2.412	0.901	2.658	4000	2.412	0.950	2.659
	$+\infty$	2.411	0.900	2.650	$+\infty$	2.411	0.950	2.650
	100	3.060	0.928	3.227	100	3.057	0.966	3.239
4. Normal	400	3.015	0.913	3.020	400	3.014	0.957	3.022
	1000	3.005	0.906	2.965	1000	3.007	0.953	2.966
	4000	3.001	0.903	2.933	4000	3.001	0.954	2.933
	$+\infty$	3.000	0.900	2.912	$+\infty$	3.000	0.950	2.912
	100	3.334	0.930	3.382	100	3.337	0.967	3.400
6. Student- t_5	400	3.276	0.909	3.160	400	3.275	0.957	3.164
	1000	3.267	0.904	3.106	1000	3.266	0.953	3.107
	4000	3.261	0.901	3.077	4000	3.261	0.951	3.077
	$+\infty$	3.260	0.900	3.060	$+\infty$	3.260	0.950	3.060
	100	3.949	0.927	3.772	100	3.945	0.965	3.791
8. Student- t_2	400	3.850	0.906	3.503	400	3.853	0.954	3.507
	1000	3.831	0.903	3.446	1000	3.834	0.953	3.449
	4000	3.823	0.901	3.423	4000	3.822	0.951	3.424
	$+\infty$	3.820	0.900	3.422	$+\infty$	3.820	0.950	3.422
	100	5.806	0.905	4.996	100	5.797	0.948	5.031
10. Cauchy	400	5.523	0.900	4.585	400	5.525	0.948	4.595
	1000	5.473	0.899	4.488	1000	5.471	0.948	4.492
	4000	5.446	0.900	$2^{1}_{4.459}$	4000	5.448	0.948	4.459
	$+\infty$	5.438	0.900	4.473	$+\infty$	5.438	0.950	4.473

Table 5: Estimates of coverage probabilities and widths of nominal 90% and 95% distribution-free confidence intervals for $\kappa_r = \kappa_{p(r),r}$ when r = 1/3 and $p(r) = \Phi(3\Phi^{-1}(r)) \approx 0.1$, for selected asymmetric models. Notation as in Table 4.

	90%				95%			
F	n	$\hat{\kappa}_{1/3}$	cp	\widehat{rw}	n	$\hat{\kappa}_{1/3}$	cp	\widehat{rw}
	100	3.124	0.924	3.380	100	3.127	0.963	3.398
12. χ_5^2	400	3.076	0.908	3.189	400	3.076	0.955	3.194
	1000	3.066	0.902	3.147	1000	3.066	0.954	3.148
	4000	3.060	0.902	3.125	4000	3.061	0.951	3.125
	$+\infty$	3.060	0.900	3.115	$+\infty$	3.060	0.950	3.115
	100	3.279	0.911	3.654	100	3.283	0.966	3.676
14. χ_2^2	400	3.217	0.901	3.494	400	3.220	0.957	3.499
	1000	3.206	0.897	3.461	1000	3.209	0.953	3.468
	4000	3.202	0.899	3.457	4000	3.202	0.954	3.458
	$+\infty$	3.200	0.900	3.474	$+\infty$	3.200	0.950	3.474
	100	3.912	0.900	4.230	100	3.911	0.945	4.249
16. Lognormal	400	3.821	0.893	4.083	400	3.820	0.945	4.084
	1000	3.802	0.895	4.052	1000	3.801	0.948	4.059
	4000	3.792	0.897	4.059	4000	3.792	0.950	4.059
	$+\infty$	3.789	0.900	4.089	$+\infty$	3.789	0.950	4.089
	100	4.394	0.927	4.729	100	4.397	0.932	4.772
18. $Pareto(2)$	400	4.264	0.906	4.634	400	4.261	0.939	4.639
	1000	4.232	0.903	4.599	1000	4.235	0.943	4.607
	4000	4.220	0.901	4.611	4000	4.221	0.946	4.611
	$+\infty$	4.216	0.900	4.652	$+\infty$	4.216	0.950	4.652
	100	5.831	0.847	_	100	5.817	0.900	_
19. Skew- $t_{2,1}$	400	5.527	0.868	5.852	400	5.525	0.922	5.874
	1000	5.471	0.883	5.775	1000	5.473	0.932	5.770
	4000	5.447	0.893	5.794	4000	5.448	0.943	5.794
	$+\infty$	5.438	$0.900^{\frac{1}{2}}$	$^{22}_{5.831}$	$+\infty$	5.438	0.950	5.831

In Table 4 are shown the results of 40,000 simulations from 5 symmetric models with sample sizes ranging from 100 to 4000. For each replicate $\hat{\kappa}_{1/3}$ and the VST constants a_0, a_1 and a_2 of (4) were also estimated, and a confidence interval found using (8) with these estimated constants. The average value of these estimates $\hat{\kappa}_{1/3}$ is shown in Column 3 of Table 4. Note the positive bias for smaller n. Despite this bias, the empirical coverage probabilities of $\kappa_{1/3} = 2.411$ in Column 4 are only slightly conservative for $n \geq 100$. To obtain the estimates of rw_{asym} shown in Column 5, we found the average of $\hat{rw}_{asym} = \sqrt{n} (rW)/z_{0.95}$, where $rW = (U - L)/\hat{\kappa}_{1/3}$, see formulae (9). Note that these estimates are also converging to their limiting value, shown in the last row for each model, and obtained from Table 3. Similar results are found for 95% confidence intervals, listed in the right hand columns of Table 4.

For simulated data generated from the normal and Student- t_5 models with sample sizes 100 the coverage probabilities are conservative, but for 400 or more the coverages and widths are reflecting our expectations. For heavier tailed distributions such as the Student- t_2 and Cauchy distributions, the methods can fail to work at all for the smaller sample sizes. This is because outliers in the samples can undermine the estimates of the sparsity index, occasionally leading to negative values of $\widehat{D}^2 = 4\hat{a}_0\hat{a}_2 - \hat{a}_1^2$.

R software functions for finding the VST constants and the resulting distribution-free confidence intervals are available online, see Section 6.

In Table 5 the results of similar studies for five asymmetric models are presented. Again, $\hat{\kappa}_{1/3}$ is biased upwards, but converges to its

target $\kappa_{1/3}$. Now the sample sizes $n \geq 400$ appear necessary to obtain 90 or 95% confidence intervals, as the case may be. For n = 100 and Model 19, no empirical average widths are tabled for the reasons just given in the last paragraph. For Model 19, which has the same kurtosis as Model 10, at least 40 times as many observations are required to obtain accurate coverage. Thus estimating $\kappa_{1/3}$ can be costly for very skewed distributions.

4.2 Power of $\hat{\pi}_{q,r}$ for Detecting Bimodality

In this section we illustrate the power of $\hat{\pi}_{q,r}$ to detect bimodality, as well as peakedness. In Section 2.1 it was shown that the extended Horn's peakedness measure defined in (1) is monotone in $\pi_{q,r}$ via (2). Recall that η_q lies in [-1,1] with negative values indicating 'bimodality', positive values 'peakedness' and 0 'uniformity' near the median. Therefore a two-sided test of $\eta_q = 0$ is approximately a two-sided test of $\pi_{q,r} = (1-2q)/(1-2r)$.

Fix q=1/4, r=3/8. In Figure 3 is shown the empirical power of the level-0.05 test of $\pi_{1/4,3/8}=2$, when the data are generated from the symmetric Beta (β,β) model, for selected values of β . The power for n=50 is shown as a dotted line, for n=200 as a dashed line and for n=800 as a solid line. These curves are near 0.05 when $\beta=1$, (the uniform model). For example, the power of detecting the bimodal model Beta(1/3,1/3) is approximately 0.4 for n=200 and 0.8 for n=800 observations. There is not much power for detecting peakedness for large β because the Beta (β,β) model approaches the Normal as $\beta \to \infty$.

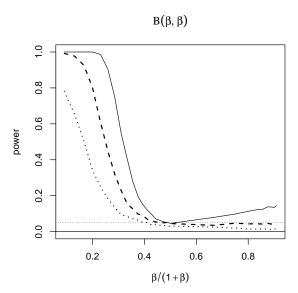


Figure 3: Graphs of empirical power of two-sided level-0.05 tests for the Beta(β , β) model plotted as a function of $\beta/(\beta+1)$. The power for n=50 is shown as a dotted line, for n=200 as a dashed line and for n=800 as a solid line. The dotted horizontal line gives the level of the test.

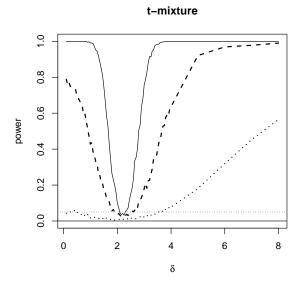


Figure 4: As in Figure 3, but now for a 50:50 mixture of two $t_{1/2}$ distributions that are distance δ apart.

Figure 4 shows the empirical power of the same distribution-free test for detecting peakedness and bimodality of a 50:50 mixture of two central $t_{1/2}$ distributions, as a function of the distance δ between them. For sample size n=200 the test has the right level and the power to detect either peakedness or bimodality, as the case may be, depending on the value of δ .

5 FURTHER RESEARCH

We extended the peakedness measure of Horn (1983) to arbitrary densities and showed that the ratio of interquantile ranges of Ruppert (1987) is approximately monotone in it when applied to the central portion of the distribution; that is, for $\pi_{q,r}$, where $q = \Phi^{-1}(-1) \approx 0.16$ or q = 0.25, say, and q < r < 0.5. When applied to the non-central portion, Ruppert's ratio $\tau_{p,q}$ for $0 is also monotone in the practical tail index of Morgenthaler & Tukey (2000). We endorse the idea that peakedness and tail-weight are best estimated separately, because as the simple factorization <math>\kappa_{p,r} = \pi_{q,r}\tau_{p,q}$ shows, kurtosis is fundamentally a product of peakedness and tail-weight.

Distribution-free confidence intervals are derived for $\kappa_{p,r}$, and hence available for $\pi_{q,r}$ and $\tau_{p,q}$ separately. In our simulation studies we concentrated on estimation of $\kappa_{1/10,1/3}$, and shown that it is possible to obtain accurate 90% and 95% distribution-free confidence intervals for data simulated from a large variety of distributions, provided that the sample sizes were at least 400. This procedure is resistant to almost 10% outliers on either side of the sample. A formula for choosing the sample size required to obtain intervals of a given desired relative

width over a large class of models is included.

Schmid & Trede (2003) found finite-sample and asymptotic tests for normality based on $\hat{\pi}_{1/8,1/4}$, $\hat{\tau}_{1/40,1/8}$ and $\hat{\kappa}_{1/40,1/4}$, using the asymptotic bivariate normality of the sample interquantile ranges. The VST-transformed pair $(K_1, K_2) = (\mathcal{K}_{\pi_0}(\hat{\pi}_{q,r}), \mathcal{K}_{\tau_0}(\hat{\tau}_{p,q}))$, where \mathcal{K} is of the form (6), is also asymptotically bivariate normal, with a covariance structure dependent on the sparsity indices at six quantiles. Thus it should be possible to find $100(1-\alpha)\%$ distribution-free confidence ellipses for the transformed pair $(\mathcal{K}_{\pi_0}(\pi_{q,r}), \mathcal{K}_{\tau_0}(\tau_{p,q}))$, and, by backtransformation, non-elliptical confidence regions for $(\pi_{q,r}, \tau_{p,q})$.

These methods can be used to find confidence intervals for the octile based kurtosis measure of Moors (1988) and the quintile based kurtosis of Jones et al. (2011), and it would be of interest to see whether or not they perform better than those presented here. A closely related problem is the estimation of tail-indices, and these methods can be easily adapted to find confidence intervals for the robust measures of tail weights proposed by Brys et al. (2006). Extensions of these inferential methods to the multivariate setting are also of interest, see Wang & Serfling (2005).

6 SUPPLEMENTARY MATERIAL

Given a vector of data x, selected values $0 , and <math>\alpha$, this script will enable the user to find a $100(1-\alpha)\%$ distribution-free confidence interval for Ruppert's measure of kurtosis $\kappa_{p,r}$, and hence also for the peakedness measure $\pi_{q,r}$ or the tail-weight measure $\tau_{p,q}$.

findDFcikurt: R script

References

- BALANDA, K.P., & MACGILLIVRAY, H.L. 1988. Kurtosis: a critical review. *The American Statistician*, **42**, 111–119.
- Balanda, K.P., & Macgillivray, H.L. 1990. Kurtosis and spread.

 The Canadian Journal of Statistics, 18, 17–30.
- BRYS, G., Hubert, M., & Struyf, A. 2006. Robust measures of tail weight. *Computational Statistics and Data Analysis*, **50**, 733–759.
- Croux, C., & Haesbroeck, G. 2001. Maxbias curves of robust scale estimates based on subranges. *Metrika*, **53**, 101–122.
- DASGUPTA, A. 2006. Asymptotic Theory of Statistics and Probability. Springer. DOI: 10.1007/978-0-387-75971-5.
- David, H. A. 1981. Order Statistics. New York: Wiley.
- GROENEVELD, R.A. 1998. A class of quantile measures for kurtosis.

 The American Statistician, 52, 325–329.
- Groeneveld, R.A., & Meeden, G. 1984. Measuring skewness and kurtosis. *The Statistician*, **33**, 391–399.
- Gupta, M.K. 1967. An asymptotically nonparametric test of symmetry. The Annals of Mathematical Statistics, 38(3), 849–866.
- HORN, P.S. 1983. A measure for peakedness. *The American Statistician*, **37**, 55–56.
- Johnson, N.L., Kotz, S., & Balakrishnan, N. 1994. *Continuous Univariate Distributions*. Vol. 1. New York: Wiley.
- Johnson, N.L., Kotz, S., & Balakrishnan, N. 1995. Continuous Univariate Distributions. Vol. 2. New York: Wiley.

- Jones, M.C., Rosco, J.F., & Pewsey, A. 2011. Skewness-invariant measures of kurtosis. *The American Statistician*, **65**(2), 89–95.
- Kotz, S., & Seier, E. 2009. An analysis of quantile measures of kurtosis. *Statistical Papers*, **50**, 553–568.
- LAWRENCE, M.J. 1975. Inequalities of s-ordered distributions. *The Annals of Statistics*, **3**, 413–428.
- Moors, J.J.A. 1988. A quantile alternative for kurtosis. *Journal of the Royal Statistical Society, Series D*, **37**, 25–32.
- MORGENTHALER, S., & TUKEY, J.W. 2000. Fitting quantiles: doubling, HR, HQ and HHH distributions. *Journal of Computational and Graphical Statistics*, **9**, 180–195.
- OJA, H. 1981. On location, scale, skewness and kurosis of univariate distributions. Scandinavian Journal of Statistics, 8, 154–168.
- Pearson, K. 1905. Skew variation, a rejoinder. *Biometrika*, 4, 169–212.
- PEWSEY, A. 2005. The large sample distribution of the most fundamental of statistical summaries. *Journal of Statistical Planning* and Inference, **134**, 434–444.
- Rosco, J.F., Jones, M.C., & Pewsey, A. 2011. Skew t distributions via the sinh-arcsinh transformation. *Test*, **20**(3), 630–652.
- RUPPERT, D. 1987. What is kurtosis? an influence function approach.

 The American Statistician, 41(1), 1–5.
- Schmid, F., & Trede, M. 2003. Simple tests for peakedness, fat tails and leptokkurtosis based on quantiles. *Computational Statistics and Data Analysis*, **43**, 1–12.

- Seier, E., & Bonett, D. 2003. Two families of kurtosis measures.

 Metrika, 58, 59–70.
- Staudte, R.G. 2013a. Inference for the standardized median. *Pages* 353–363 of: Lahiri, S., Schick, A., Sengupta, A., & Sriram, N.T. (eds), *Contemporary developments in statistical theory; a Festscrift in honour of Professor Hira Lal Koul.* Springer.
- STAUDTE, R.G. 2013b. Distribution-free confidence intervals for the standardized median. *STAT*, **2**(1), 184–196.
- STAUDTE, R.G. 2014. Inference for quantile measures of skewness.

 Test. To appear; DOI:10.1007/s11749-014-0391-5.
- TEAM, R DEVELOPMENT CORE. 2008. R: A language and environment for statistical computing. R Foundation for Statistical Computing, Vienna, Austria. ISBN 3-900051-07-0.
- Tukey, J.W. 1965. Which part of the sample contains the information? *Proceedings of the Mathemetical Academy of Science USA*, **53**, 127–134.
- VAN ZWET, W.R. 1964. Transformations of random variables. Amsterdam: Math. Zentrum.
- Wang, J., & Serfling, R. 2005. Nonparametric multivariate kurtosis and tailweight measures. *Nonparametric Statistics*, **17**, 441–456.
- WITHERS, C.S., & NADARAJAH, S. 2011. Bias-reduced estimates for skewness, kurtosis, L-skewness and L-kurtosis. *Journal of Statistical Planning and Inference*, **141**, 3839–3861.